THE JOURNAL OF BIOLOGICAL CHEMISTRY VOL. 282, NO. 16, pp. 12176–12185, April 20, 2007
Printed in the U.S.A.

Relocalization of STIM1 for Activation of Store-operated Ca^{2+} Entry Is Determined by the Depletion of Subplasma Membrane Endoplasmic Reticulum Ca^{2+} Store*[S]

Received for publication, October 5, 2006, and in revised form, January 16, 2007 Published, JBC Papers in Press, February 12, 2007, DOI 10.1074/jbc.M609435200

Hwei Ling Ong[‡], Xibao Liu[‡1], Krasimira Tsaneva-Atanasova[§1], Brij B. Singh[¶], Bidhan C. Bandyopadhyay[‡], William D. Swaim[‡], James T. Russell[‖], Ramanujan S. Hegde[**], Arthur Sherman[§], and Indu S. Ambudkar[‡2]

From the [‡]Secretory Physiology Section, Gene Therapy and Therapeutics Branch, NIDCR, National Institutes of Health, Bethesda, Maryland 20892, the [¶]Department of Biochemistry and Molecular Biology, School of Medicine and Health Sciences, University of North Dakota, Grand Forks, North Dakota 58203, the [**]Cell Biology and Metabolism Branch and [‖]Microscopy and Imaging Core, NICHD, National Institutes of Health, Bethesda, Maryland 20892, and the [§]Laboratory of Biological Modeling, NIDDK, National Institutes of Health, Bethesda, Maryland 20892

STIM1 (stromal interacting molecule 1), an endoplasmic reticulum (ER) protein that controls store-operated Ca^{2+} entry (SOCE), redistributes into punctae at the cell periphery after store depletion. This redistribution is suggested to have a causal role in activation of SOCE. However, whether peripheral STIM1 punctae that are involved in regulation of SOCE are determined by depletion of peripheral or more internal ER has not yet been demonstrated. Here we show that Ca^{2+} depletion in subplasma membrane ER is sufficient for peripheral redistribution of STIM1 and activation of SOCE. 1 μM thapsigargin (Tg) induced substantial depletion of intracellular Ca^{2+} stores and rapidly activated SOCE. In comparison, 1 nM Tg induced slower, about 60–70% less Ca^{2+} depletion but similar SOCE. SOCE was confirmed by measuring I_{SOC} in addition to Ca^{2+}, Mn^{2+}, and Ba^{2+} entry. Importantly, 1 nM Tg caused redistribution of STIM1 only in the ER-plasma membrane junction, whereas 1 μM Tg caused a relatively global relocalization of STIM1 in the cell. During the time taken for STIM1 relocalization and SOCE activation, 1 nM Bodipy-fluorescein Tg primarily labeled the subplasma membrane region, whereas 1 μM Tg labeled the entire cell. The localization of Tg in the subplasma membrane region was associated with depletion of ER in this region and activation of SOCE. Together, these data suggest that peripheral STIM1 relocalization that is causal in regulation of SOCE is determined by the status of $[Ca^{2+}]$ in the ER in close proximity to the plasma membrane. Thus, the mechanism involved in regulation of SOCE is contained within the ER-plasma membrane junctional region.

Store-operated calcium entry (SOCE)[3] is activated in response to depletion of Ca^{2+} in intracellular Ca^{2+} store(s). SOCE not only ensures refilling of the intracellular Ca^{2+} stores but also provides sustained elevation of cytosolic $[Ca^{2+}]$ ($[Ca^{2+}]_i$). Physiologically, SOCE is activated by agonist-stimulated generation of inositol 1,4,5-trisphosphate (IP_3) and IP_3-mediated release of Ca^{2+} from ER Ca^{2+} stores via the IP_3 receptor. It has been clearly demonstrated that during refilling of internal Ca^{2+} stores, Ca^{2+} entering the cell is rapidly taken up into the ER by SERCA activity with minimal diffusion in the subplasma membrane region. These studies indicate close apposition of the ER and plasma membrane at the site of SOCE (1–6). Thus, it has been suggested that ER localized in the subplasma membrane region is likely to be coupled to SOCE and that depletion of these local Ca^{2+} stores triggers activation of SOCE. The presently proposed mechanisms for activation of SOCE suggest direct physical coupling between components in the ER and plasma membrane, generation of diffusible components, or recruitment of the SOC channel. The exact mechanism involved in regulation of SOCE as well as the molecular components of the channel(s) mediating Ca^{2+} entry in different types of cells has not been clearly identified.

Recent studies have suggested STIM1 (stromal interacting molecule 1) as a novel regulator for SOCE. STIM1, which is a Ca^{2+}-binding protein localized diffusely in the ER, has been shown to relocate into a peripheral region of the cell in response to internal Ca^{2+} store depletion (7, 8). STIM1 displays punctate subplasma membrane localization in response to depletion of intracellular Ca^{2+} stores, which has been reported to be causal in activation of SOCE and to define the elementary unit that is involved in SOCE. Although several studies have clearly established involvement of ER-plasma membrane junctional domains in the regulation of SOCE, the exact site of store depletion has not yet been demonstrated. Based on all of the data available presently, it is logical to propose that that since the EF-hand domain of STIM1 is localized in the lumen of the ER and STIM1 punctae involved in SOCE activation are localized in subplasma membrane Ca^{2+} stores very close to the surface

* The costs of publication of this article were defrayed in part by the payment of page charges. This article must therefore be hereby marked "*advertisement*" in accordance with 18 U.S.C. Section 1734 solely to indicate this fact.

[S] The on-line version of this article (available at http://www.jbc.org) contains supplemental Figs. 1 and 2.

[1] These authors contributed equally to this work.

[2] To whom correspondence should be addressed: Bldg. 10, Rm. 1N-113, 10 Center Dr., National Institutes of Health, Bethesda, MD 20892. Tel.: 301-496-5298; Fax: 301-402-1228; E-mail: indu.ambudkar@nih.gov.

[3] The abbreviations used are: SOCE, store-operated Ca^{2+} entry; IP_3, inositol 1,4,5-trisphosphate; SERCA, sarcoplasmic/endoplasmic reticulum Ca^{2+} ATPase(s); ER, endoplasmic reticulum; SOC, store-operated Ca^{2+}; Tg, thapsigargin; BD-Tg, Bodipy-fluorescein thapsigargin; CCh, carbachol; 2-APB, 2-aminoethyldiphenylborinate; SES, standard extracellular solution; YFP, yellow fluorescent protein; TIRF, total internal reflection fluorescence; TIRFM, TIRF microscopy.

membrane (probably interacting with SOCE channels), this ER Ca^{2+} store would have to be depleted for activation of SOCE. Further, these stores would have to remain in a depleted state in order to retain the punctate localization of STIM1, which is required to maintain SOCE in an activated state. However, conditions typically used for activating SOCE and assessing STIM1 function (8–13) involve high concentrations of thapsigargin (Tg) or agonists that induce substantial and global depletion of internal Ca^{2+} stores. Thus, it is unclear whether changes in the local Ca^{2+} store (*i.e.* in the vicinity where regulation of SOCE seems to be taking place) regulate relocation of STIM1 and activation of SOCE or whether signals from more interior regions of the cell are required.

In this study, we have assessed whether STIM1 regulation of SOCE is dependent on the $[Ca^{2+}]$ in subplasma membrane ER or in more internal ER. We have used low concentrations of Tg to slow down the process of ER depletion and activation of SOCE. It has been previously shown that low concentrations of Tg that induce only partial depletion of internal Ca^{2+} stores result in a slow but almost complete activation of I_{CRAC} (14, 15), although these previous studies do not clarify the location of the SOCE-coupled ER Ca^{2+} store. We demonstrate that as Tg diffuses into the periphery of the cell, Ca^{2+} stores in this region are depleted, and this is associated with activation of SOCE. SOCE is not further enhanced by depletion of more internal ER. Further, we show that mobilization of the SOCE regulatory protein STIM1 in the subplasma membrane region of the cells is associated with depletion of ER in this region. Together, our data suggest that STIM1 senses $[Ca^{2+}]$ within ER localized in the ER-plasma membrane junctional regions and that the status of this peripheral ER Ca^{2+} store determines peripheral relocation of STIM1 that is required for activation of SOCE.

EXPERIMENTAL PROCEDURES

Materials—Bodipy-fluorescein thapsigargin (BD-Tg), Fura-2/AM, Mag-Fluo4AM, Fluo-4AM, and the ER-Tracker Red dye and Vybrant staining assay were obtained from Invitrogen. Tg was obtained from Calbiochem. Carbachol (CCh) and 2-aminoethyldiphenylborinate (2-APB) were obtained from Sigma. Glass-bottomed 35-mm Petri dishes were obtained from MatTek Corp. (Ashland, MA). Glass coverslips were obtained from Fisher. The rabbit antibody against phosphorylated PERK (phospho-PERK) was obtained from Cell Signaling Technology (Danvers, MA). The mouse anti-STIM1 antibody was obtained from BD Biosciences, whereas the fluorescein isothiocyanate-conjugated donkey anti-mouse antibody was from Jackson Immunoresearch (West Grove, PA). The cDNA for untagged STIM1 was obtained from OriGene (Rockville, MD).

Cell Culture and Transient Transfection—HSG cells were cultured on glass coverslips and were transiently transfected with untagged STIM1 (1 μg) or YFP-STIM1 (1 μg) for 48 h using the method described previously (16). For $[Ca^{2+}]_i$ measurements and live cell imaging experiments, cells were plated on glass-bottomed 35-mm Petri dishes. For patch clamp measurement and TIRF, cells were plated on glass coverslips.

$[Ca^{2+}]_i$ Measurements—Measurements with 1 μM Fura-2/AM and analyses of data were conducted as described previously (17, 18).

Electrophysiological Measurements—Whole cell-attached patch clamp measurements were performed as described previously (1, 17–19). For Ca^{2+} current measurements, the external solution was composed as follows: 145 mM NaCl, 5 mM CsCl, 1 mM $MgCl_2$, 10 mM $CaCl_2$, 10 mM HEPES, 10 mM glucose, pH 7.4 (NaOH). For DVF-Na^+ current measurements, the external solution was composed as follows: 165 mM NaCl, 5 mM CsCl, 10 mM EDTA, 10 mM HEPES, 10 mM glucose, pH 7.4 (NaOH). The patch pipette contained the standard intracellular solution, which was composed as follows: 145 mM cesium methane sulfonate, 8 mM NaCl, 5 mM $MgCl_2$, 10 mM HEPES, 10 mM EGTA, pH 7.2 (CsOH).

Immunodetection of Phosphorylated PERK—Lysates from HSG cells were prepared, and immunoblotting using phospho-PERK antibody was carried out as described previously (20, 21).

Immunofluorescence and Confocal Microscopy—Immunofluorescence was conducted in a similar manner as described previously (22). Cells were stained with the mouse anti-STIM1 antibody (1:100 dilution) and probed using a donkey anti-mouse antibody conjugated to fluorescein isothiocyanate (1:100 dilution). Fluorescence images were acquired using a confocal laser-scanning microscope Leica TCS-SP2 attached to an upright Leica DM-RE7 microscope as described earlier (22).

Live Cell Imaging Using BD-Tg—HSG cells were scanned using Leica TCS SP2 attached to an inverted Leica DM-IRE2 microscope. BD-Tg was added to the cells at 1 μM and 1 nM concentrations. Fluorescence intensity in selected regions of the cell was measured. Images were acquired every 3 s for 3 min. Background fluorescence was subtracted from each data point.

$[Ca^{2+}]_{ER}$ Measurements—HSG cells were loaded with 3 μM Mag-Fluo4AM in a Ca^{2+}-containing standard extracellular solution (Ca^{2+}-SES) for 1 h at 37 °C in 5% CO_2. The Ca^{2+}-SES was composed as follows: 145 mM NaCl, 5 mM CsCl, 1 mM $MgCl_2$, 1 mM $CaCl_2$, 10 mM HEPES, 10 mM glucose, pH 7.4 (NaOH) (23). After incubation, cells were then rinsed with Ca^{2+}-free SES and used in live cell imaging experiments on a Leica DM-IRE2 microscope as described above or in TIRF imaging as described below.

Vybrant Staining Assay—Vybrant staining assay was used to evaluate apoptosis, using the method described previously (24).

TIRF Imaging—HSG cells were seeded and cultured overnight on glass coverslips, which formed the base of a perfusion chamber that was mounted on the stage of an Olympus IX81 motorized inverted microscope (OPELCO, Dulles, VA). Prior to the start of imaging, cells were loaded with 4 μM Fluo-4AM in a Ca^{2+}-SES for 1 h at 37 °C in 5% CO_2. To determine ER localization in the subplasma membrane regions, cells were loaded with 1 μM ER-Tracker Red dye for 1 h at 37 °C. TIRF imaging was then conducted as described previously (25). Changes in Fluo-4 fluorescence were calculated using KaleidaGraph software (Red Rock Software, Salt Lake City, UT) and were expressed as $\Delta F/F_0$, where F is the fluorescence captured at a particular time point and F_0 is the mean fluorescence intensity from the initial 20 captured images.

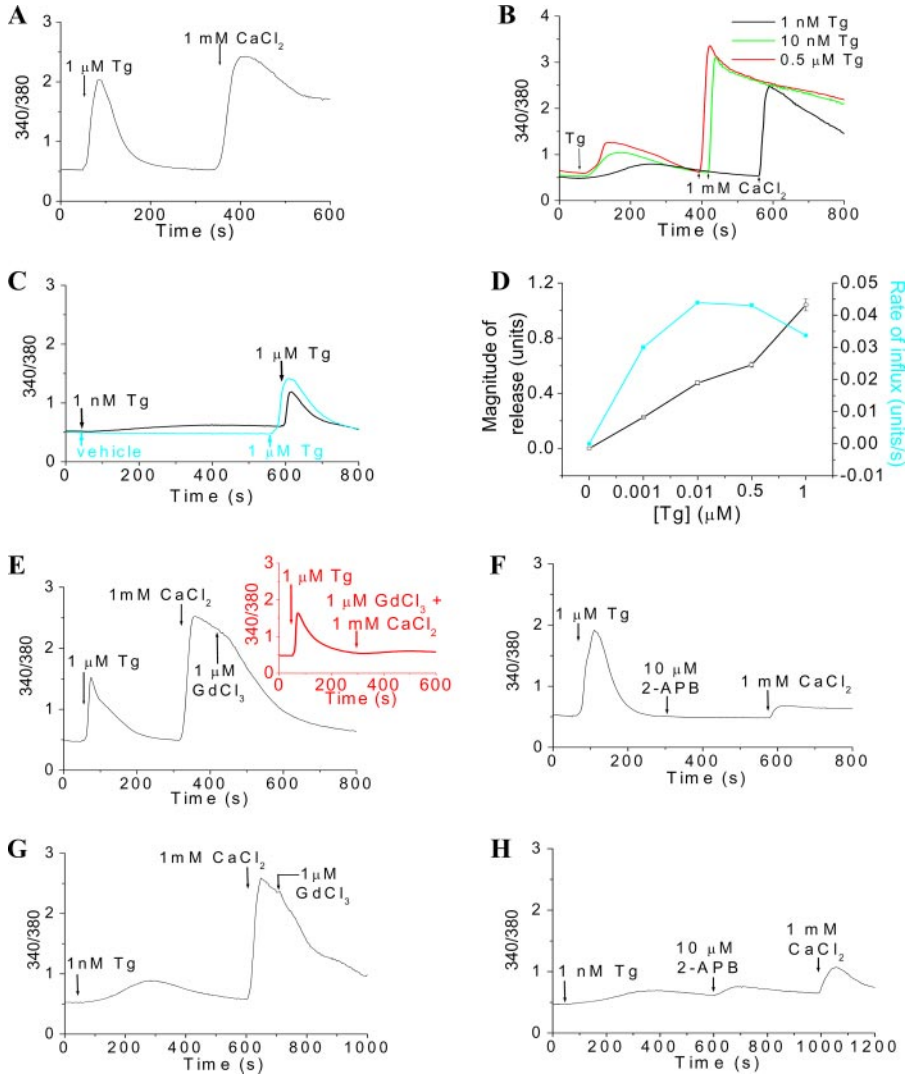

FIGURE 1. **Activation of SOCE by incomplete depletion of ER Ca^{2+} stores.** *A* and *B*, Tg-induced intracellular Ca^{2+} release and Ca^{2+} entry in HSG cells. The various [Tg] used for activation of SOCE are indicated in the figure. *C*, Ca^{2+} release induced by 1 μM Tg in control cells (*blue trace*) and in cells previously treated with 1 nM Tg (*black trace*), indicating the extent of depletion of ER by 1 nM Tg. *D*, dose-response curve showing the effect of [Tg] on Ca^{2+} release (units; *squares*) and the rate of Ca^{2+} influx (units/s; *circles*). Data were plotted as mean ± S.E. from three or four separate experiments and expressed in 340/380 fluorescence ratio units; *error bars* were within the size of the *symbols*. Ca^{2+} influxes induced by 1 μM and 1 nM Tg were blocked by 1 μM $GdCl_3$ (*E* and *G*, respectively) and 10 μM 2-APB (*F* and *H*, respectively). A trace showing the inhibition of Ca^{2+} influx induced by 1 μM Tg by 1 μM $GdCl_3$ added before 1 mM $CaCl_2$ is shown as an *inset* (similar results were seen with 1 nM Tg; data not shown) in *E*. $[Ca^{2+}]_i$ was measured in Fura-2-loaded cells and is expressed as 340/380 ratio. Each analog plot showing Ca^{2+} release and Ca^{2+} entry is representative of at least four experiments, each trace showing the average from at least 50 cells.

RESULTS

Submaximal Depletion of ER Ca^{2+} Store Activates SOCE—Stimulation of HSG cells by the endoplasmic Ca^{2+} pump inhibitor Tg (1 μM) induces an initial rapid increase in $[Ca^{2+}]_i$ (represented by the 340/380 fluorescence ratio; Fig. 1*A*) due to internal Ca^{2+} release, which is detected as a transient $[Ca^{2+}]_i$ increase in the absence of external Ca^{2+}. The addition of Ca^{2+} to the external medium after internal store depletion induces a second increase in $[Ca^{2+}]_i$ due to Ca^{2+} influx. At this concentration, Tg induces almost complete depletion of the internal IP_3-sensitive Ca^{2+} store (the addition of Tg after carbachol induced some additional Ca^{2+} release but not *vice versa*; data not shown). Further, caffeine does not affect Tg- or carbachol-induced $[Ca^{2+}]_i$ increase in HSG cells (data not shown). The contribution of mitochondrial Ca^{2+} transport to the Tg-stimulated $[Ca^{2+}]_i$ changes was not assessed.

To determine the extent of $[Ca^{2+}]_{ER}$ depletion required for activation of SOCE, we examined internal Ca^{2+} release and Ca^{2+} entry induced by lower [Tg]. 0.5 μM, 10 nM, and 1 nM Tg induced slower and less internal Ca^{2+} release than 1 μM Tg (Fig. 1*B*). Importantly, substantial Ca^{2+} entry was seen at the lower [Tg], and neither the rates nor amplitudes of the $[Ca^{2+}]$ increase at the various [Tg] were significantly different from each other (see Fig. 1*D* and also traces in Fig. 1, *E* and *G*). The extent of store depletion was assessed by the addition of 1 μM Tg after treatment of cells with lower [Tg] (Fig. 1, *C* and *D*). The 1 μM Tg-induced $[Ca^{2+}]_i$ increase was reduced by <50% in cells pretreated with 1 nM Tg for 500 s, suggesting that at least 50% of internal Ca^{2+} store was not associated with activation of Ca^{2+} entry. Similarly, 10 nM and 0.5 μM also induced less store depletion compared with 1 μM Tg (see Fig. 1*D*). These data demonstrate that Ca^{2+} entry is activated even when internal Ca^{2+} stores are incompletely depleted. To confirm that SOCE is activated by 1 nM Tg, we examined the effects of Gd^{3+} and 2-APB, both of which are used to block SOCE (26, 27). Ca^{2+} entry stimulated by 1 μM and 1 nM Tg was inhibited by 1 μM Gd^{3+} and 10 μM 2-APB (Fig. 1, *E–H*, respectively). The inhibitory effect of 1 μM Gd^{3+} was seen whether it was added before or after 1 mM $CaCl_2$ (Fig. 1*E*, *inset*; data with 1 nM Tg not shown). These findings strongly suggest that SOCE is activated under conditions where there is relatively less depletion of the ER Ca^{2+} store.

1 nM Tg, like 1 μM Tg, also activated the previously described inwardly rectifying store-operated Ca^{2+} current, I_{SOC}, in HSG cells (1) (Fig. 2, *A–C*). However, the magnitude of the current with 1 nM Tg was about 60% less than that with 1 μM Tg, and there was also a longer lag before an increase in current was detected (209 ± 55 s compared with 20 ± 4 s with 1 μM Tg). Notably, the current developed rapidly after this lag period and appeared to be quite stable, unlike the current with 1 μM Tg, which inactivated more rapidly. These data are inconsistent with the Fura-2 data, which demonstrate that 1 μM and 1 nM Tg

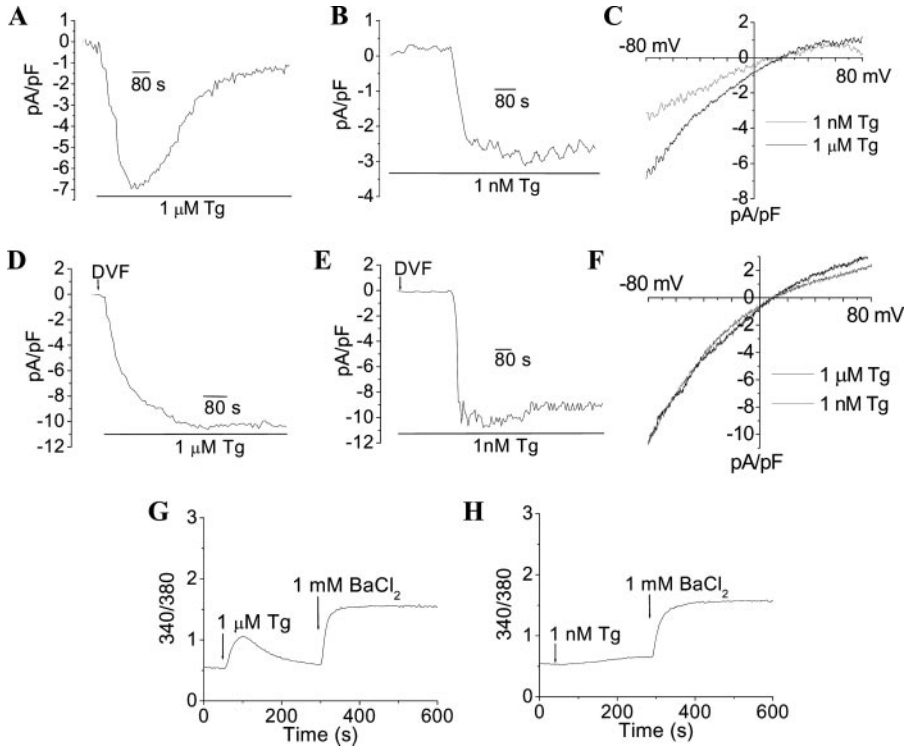

FIGURE 2. **Activation of I_{SOC} and Ba^{2+} influx by thapsigargin.** Shown is activation of I_{SOC} by high (*A*) and low [Tg] (*B*) in Ca^{2+}- and Mg^{2+}-containing external medium (currents recorded at −80 mV are plotted). *I-V* relationships of the maximum currents shown in *A* and *B* are presented in *C*. Shown is activation of I_{SOC} by high (*D*) and low [Tg] (*E*) in DVF medium (currents recorded at −80 mV are plotted). *I-V* relationships of the maximum currents in *D* and *E* are shown in *F*. These data represent results obtained with a minimum of 7–10 cells under each condition, with each trace showing the plot obtained with a single representative cell. Other details are provided under "Experimental Procedures." Shown is 1 μM (*G*) and 1 nM Tg (*H*)-induced Ba^{2+} influx. Cells were stimulated with Tg in Ca^{2+}-free medium, and 1 mM $BaCl_2$ was added where indicated. Basal Ba^{2+} entry, in unstimulated cells incubated in Ca^{2+}-free medium was minimal (data not shown).

activate similar magnitude of SOCE, although activation is slower at the lower [Tg]. We hypothesized that this discrepancy could be due to a contribution of Ca^{2+}-induced Ca^{2+} release to the Fura-2 fluorescence measurements (28). Alternatively, it could be a result of recycling of Ca^{2+} into the ER store by residual SERCA activity in cells treated with the lower [Tg]. It should be noted that since I_{SOC} measurements were done in the presence of 10 mM external Ca^{2+}, it is possible that, despite the buffering of Ca^{2+} in the pipette solution, Ca^{2+} entering the cell is taken back into the ER to partially refill the store (3). However, removal of external Ca^{2+} (as was the case in the Fura-2 assay) would allow this store to be substantially depleted. Uptake of Ca^{2+} into the ER by the residual SERCA activity in cells stimulated with low [Tg] will also result in lower ambient $[Ca^{2+}]_i$, which would attenuate Ca^{2+}-dependent inactivation of SOCE and account for the relatively stable I_{SOC} in these cells.

To determine the possible contribution of Ca^{2+} entry and ER Ca^{2+} recycling, I_{SOC} was measured in a divalent cation-free external medium (Figs. 2, *D–F*). Under these conditions, (i) the magnitudes of the steady-state currents induced by 1 nM and 1 μM Tg were similar, and (ii) the lag time for current activation with 1 nM Tg was reduced (140 compared with 209 s). The possible contribution of Ca^{2+}-induced Ca^{2+} release was confirmed by measuring Ba^{2+} entry stimulated by 1 nM or 1 μM Tg. As seen in the traces shown in Fig. 2, *G* and *H*, similar levels of Ba^{2+} entry were induced under the two conditions (basal Ba^{2+} entry into these cells was not detectable). In aggregate, these data suggest that Ca^{2+} entry and reuptake into ER account for the lower magnitude and in part for the longer lag time for activation of I_{SOC} (with Ca^{2+} as the charge carrier) in cells treated with 1 nM Tg. The longer lag for activation of I_{SOC} at the lower [Tg] is also due to the longer diffusion time and probably reflects the time required to inhibit enough SERCA to achieve sufficient depletion of ER Ca^{2+}. Once this is achieved, I_{SOC} is rapidly activated.

The relatively slow internal Ca^{2+} release induced by 1 nM Tg allowed us to examine the temporal characteristics of SOCE activation. The readdition of external Ca^{2+} at 20, 50, 150, and 250 s after stimulation with 1 nM Tg in Ca^{2+}-free medium resulted in substantial elevations of $[Ca^{2+}]_i$ (Figs. 3, *A–D*, respectively), which was blocked by 2-APB (Fig. 3*C*, *dashed line*). Fig. 3*E* demonstrates that SOCE is half-maximally activated within 20 s and maximally activated by 150 s. The magnitude of SOCE activated by 1 nM Tg at 150 s was similar to that activated by 1 μM Tg for 300 s (*asterisk* in Fig. 3*E*). Note that longer incubation with either the low or high Tg did not induce any further increase in SOCE. The addition of 1 μM Tg after stimulation with 1 nM Tg for 150 s demonstrated that there was about 30% depletion of the internal Ca^{2+} store (data not shown, but compare with Fig. 1*C*). Together, these data demonstrate that SOCE is maximally activated by 150 s after 1 nM Tg treatment. To confirm this, SOCE was measured using Mn^{2+} as a Ca^{2+} surrogate (29). 50 s after the addition of 1 nM Tg, the rate of Fura-2 quenching was substantially less than that induced by 1 μM Tg (Fig. 3*F*). However, similar Mn^{2+} entry was seen in cells stimulated for 150 and 250 s with either 1 nM or 1 μM Tg (Fig. 3, *G* and *H*). In aggregate, these data suggest that depletion of SOCE-coupled stores with 1 nM Tg is slow at first due to recycling of Ca^{2+} into the ER by residual SERCA activity. This would also account for the transient increase in $[Ca^{2+}]_i$ at the 20 s time point (Fig. 3*A*). With time enough, SERCA are inactivated to prevent this recycling, thus resulting in complete activation of SOCE (similar magnitude seen with 1 nM Tg and 1 μM Tg).

Translocation of STIM1 by Low and High Concentrations of Thapsigargin—STIM1 has been proposed to be an essential regulatory protein for SOCE (10–13). It is translocated to the plasma membrane region of cells upon depletion of internal Ca^{2+} stores, and this translocation has been associated with activation of SOCE. We have used TIRFM to examine localization of heterologously expressed YFP-STIM1 in HSG cells.

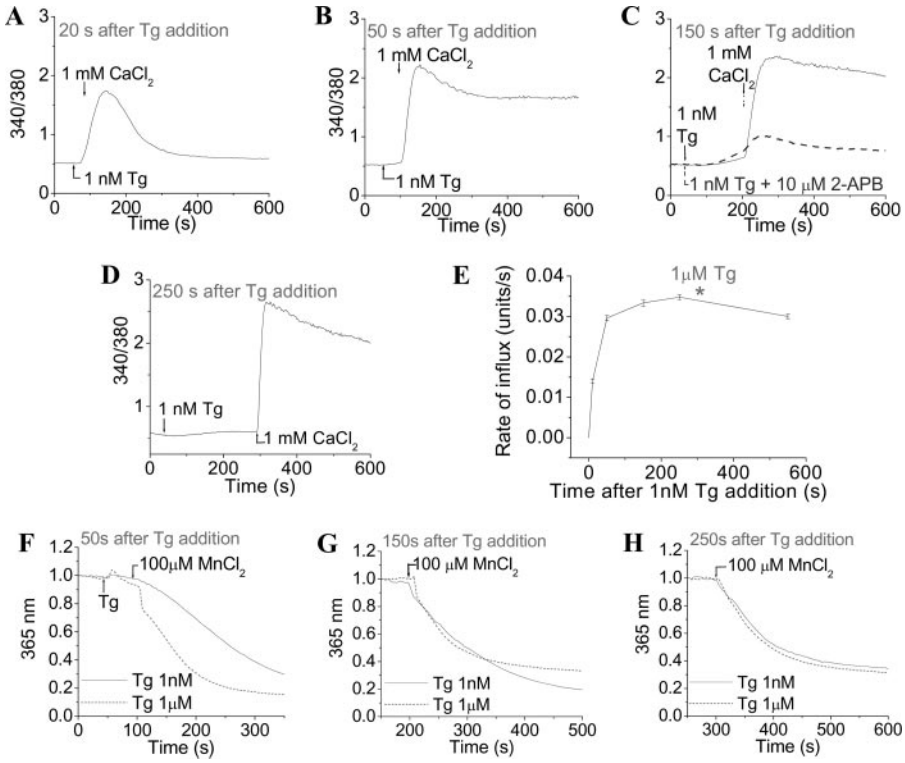

FIGURE 3. **Temporal characteristics of SOCE activation.** Cells were stimulated with 1 nM Tg in Ca^{2+}-free medium. 1 mM $CaCl_2$ was added at 20 (*A*), 50 (*B*), 150 (*C*), and 250 s (*D*) after the Tg addition. *E*, time course of SOCE activation upon Ca^{2+} addition after 1 nM Tg (rate of Ca^{2+} influx (units/s) *versus* time (s) after 1 nM Tg addition). The *asterisk* shows the rate of maximal Ca^{2+} influx (units/s) induced by 1 μM Tg with 1 mM $CaCl_2$ added 300 s after the Tg addition. Data are plotted as mean ± S.E. ($n = 3$). Mn^{2+} influx was induced by 1 μM (*dotted line*) and 1 nM Tg (*solid line*). Cells were stimulated with Tg in Ca^{2+}-free medium, and 100 μM $MnCl_2$ was added 50 (*F*), 150 (*G*), and 250 s (*H*) after the addition of Tg. Relative fluorescence at 365 nm is shown (these traces represent average fluorescence changes from more than 70 cells. Similar results were obtained in four separate experiments).

Depletion of Peripheral Ca^{2+} Stores Is Associated with STIM1 Relocation and SOCE Activation—We assessed the localization of the ER stores involved in STIM1 regulation of SOCE by using several different experimental protocols. First, BD-Tg and live cell confocal imaging were used to determine the extent of diffusion (and thus localization) of Tg in HSG cells during activation of SOCE. 1 μM BD-Tg rapidly induced strong labeling of all of the ER (Fig. 5*B*, *top*, shows *x–y image*). The *x–z* image (Fig. 5*B*, *bottom*) demonstrates that this labeling is predominantly perinuclear. In comparison, the pattern of labeling seen with 1 nM BD-Tg was quite distinct. Strong punctate labeling was seen only in the subplasma membrane region (Fig. 5*A*, *top*, shows *x–y image*) with very little intracellular fluorescence. This was confirmed by the *x–z* image of the cells (Fig. 5*A*, *bottom*), which clearly shows the peripheral localization of this signal. Overlay of Bodipy-fluorescein and differential interference contrast images of selected cells are shown in Fig. 5*C*. Further, specificity of labeling was assessed by preincubation of cells with 2 nM Tg for 3 min before treatment with 1 nM BD-Tg. This preincubation dampened the labeling of the cells with BD-Tg (Fig. 5*D*; at higher [BD-Tg], initial fluorescence was similarly dampened by preincubation of cells with an equivalent concentration of nonfluorescent Tg). Fluorescence was measured in selected regions of the cell following stimulation with 1 nM Tg (Fig. 5*E*) (images were collected up to 3 min, and data from the first 150 s are shown; note that SOCE was maximally activated by 1 nM Tg within 150 s). BD-Tg fluorescence in the subplasma membrane region increased within the 5 s after Tg addition and continued to rise, leveling out at after 150 s. Signal in the nucleus did not significantly increase until about 100 s. Fluorescence in the internal region was less than in the subplasma membrane ER and displayed a slow, somewhat linear increase after a longer initial lag. Thus, with 1 nM BD-Tg, initial labeling was mostly limited to the subplasma membrane region of the cell, suggesting that SOCE activation by 1 nM Tg is coincident with the presence of Tg in the subplasma membrane region of the cell. With time, there was further diffusion of Tg into the more internal region of the cell and more global inactivation of SERCA in the cells but without a corresponding increase in SOCE. The peripheral localization of 1 nM BD-Tg during activation of Ca^{2+} entry suggests that the ER in this region is depleted rather than the more internal ER. This was examined using a mathematical model based on the data in Fig. 5 and in a

Both low and high concentrations of Tg stimulated movement of YFP-STIM1 in the subplasma membrane in cells maintained in a Ca^{2+}-containing medium in contrast to control cells expressing mYFP alone, which does not change (Fig. 4*A*). However, although there was a fast and almost uniform increase in STIM1 punctae with 1 μM Tg (Fig. 4*B*; punctae were detected at 2 min and maximum by 4 min), translocation of STIM1 with 1 nM Tg (Fig. 4*C*) was relatively slower (4 and 6 min time points are shown). The addition of 1 μM Tg after 1 nM Tg to these cells induced a further increase in STIM1 in the subplasma membrane region (data not shown). Importantly, when cells were treated with 1 nM Tg in the absence of external Ca^{2+}, the extent of STIM1 relocalization was similar to that induced by 1 μM Tg (Fig. 4*D*). The data in Fig. 4, *B–D*, are fully consistent with the functional data shown in Figs. 1–3. In the presence of 1 nM Tg, rapid recycling of Ca^{2+} that enters cells incubated in a Ca^{2+}-containing medium prevents complete depletion of the ER Ca^{2+} store, thus accounting for the lower SOCE and less STIM1 redistribution into punctae. When Ca^{2+} is removed from the external solution, the store depletes more substantially, and thus when Ca^{2+} is readded to the external medium, comparable influx is seen in the two conditions. These data clearly demonstrate that incomplete depletion of ER Ca^{2+} stores is sufficient for relocalization of STIM1 and activation of SOCE.

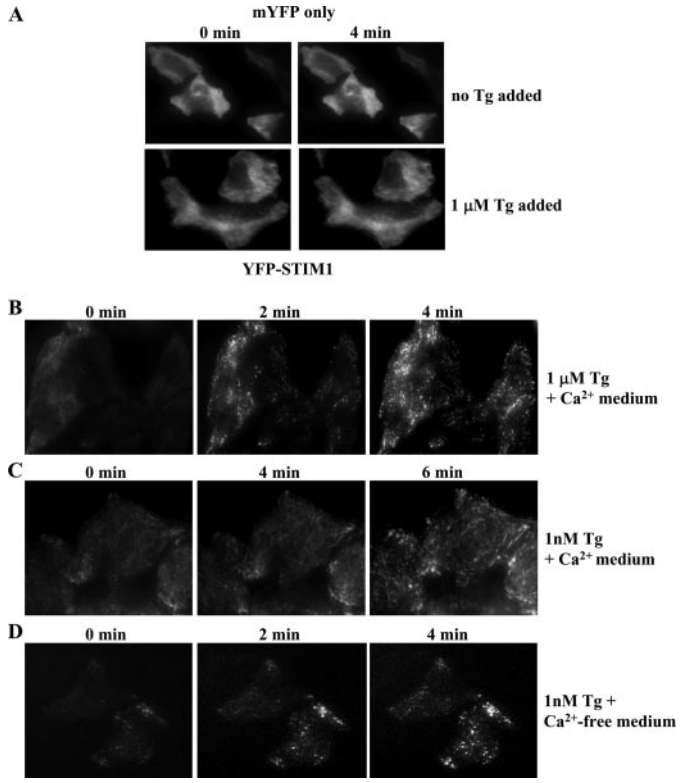

FIGURE 4. **Redistribution of YFP-STIM1 to the subplasma membrane region following Tg stimulation.** *A*, distribution of mYFP, measured using TIRFM in control and Tg-treated cells. *B* and *C*, redistribution of YFP-STIM1 following stimulation with 1 μM and 1 nM Tg, respectively, in Ca^{2+}-containing medium. *D*, redistribution of YFP-STIM1 following stimulation with 1 nM Tg in Ca^{2+}-free medium. The time point at which each image was taken is noted in the figure.

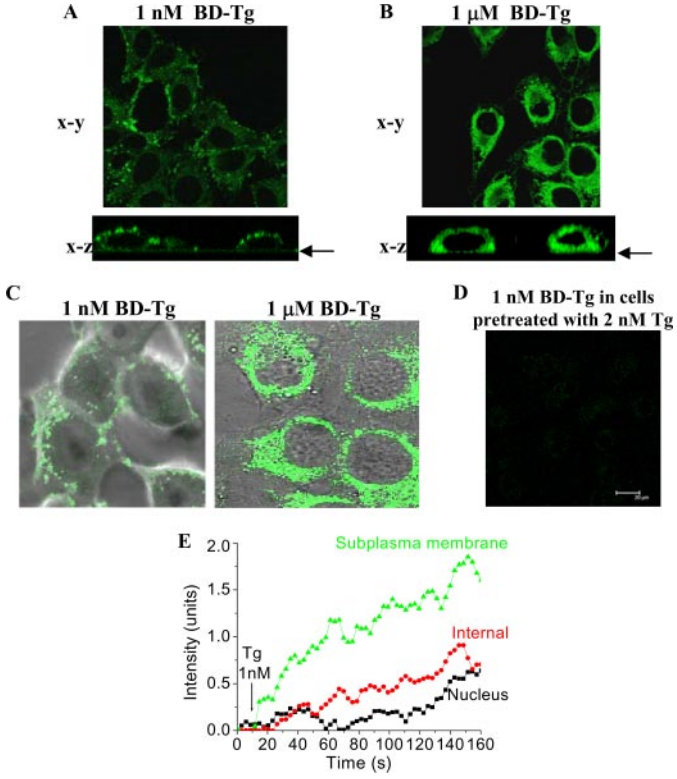

FIGURE 5. **Localization of Tg during activation of SOCE.** *A* and *B*, labeling of HSG cells with 1 nM and 1 μM BD-Tg detected by confocal microscopy. The images shown were taken 3 min after the addition of BD-Tg and displayed along the *x-y* (*top*) and *x–z* (*bottom*) axes. The *arrow* shows the bottom of the dish (*C*). Overlays of BD-Tg labeled cells and the differential interference contrast images of the same field. *D*, dampening of the BD-Tg signal when 1 nM BD-Tg was added following preincubation of cells with 2 nM unlabeled Tg. *E*, time course of labeling the subplasma membrane, internal, and nuclear regions with 1 nM BD-Tg. Quantification was done as described under "Experimental Procedures" using specific regions of interest in the areas of the cell indicated. Similar data were obtained from five separate experiments.

previous report (15). We wanted to test whether a model with two ER compartments that are functionally distinct but slowly equilibrate with each through diffusion of Ca^{2+} between them (see supplemental materials for details) could account for the data in Fig. 3, *A–C*. Supplemental Fig. 1, *A–C*, confirms that this simple model reproduces those observation. The simulations further predict (supplemental Fig. 1, *D–F*) that when cells are treated with 1 nM Tg, there is greater depletion of the local subplasma membrane Ca^{2+} store than the internal ER within the time frame for activation of Ca^{2+} entry. Thus, the simulations agree well with our hypothesis that activation of Ca^{2+} entry is associated with the depletion of peripheral ER Ca^{2+} stores.

This was directly confirmed by measuring the depletion of Ca^{2+} stores in the subplasma membrane region of the cells ($[Ca^{2+}]_{ER}$) by using Mag-Fluo4 and confocal microscopy. Images of the whole cell were taken, and changes in the fluorescence of selected regions of interest in the cell were determined. 1 nM or 1 μM Tg induced a faster decrease of the fluorescence in the subplasma membrane region ER (ER_{sub}) than in the internal ER (Fig. 6, *A* and *B*; Fig. 6*C* shows fluorescence in unstimulated cells). Furthermore, the decrease with 1 μM Tg in both ER regions was faster than with 1 nM Tg. It should be noted that the decrease in Mag-Fluo4 fluorescence (representing ER $[Ca^{2+}]$) is relatively slower than the increase in Fura-2 fluorescence (representing $[Ca^{2+}]_i$) under the same conditions. This difference is most likely due to the higher $[Ca^{2+}]$ in ER compared with the cytosol. Thus, the relative changes in fluorescence are larger in the cytosol than in the ER. A similar slow decrease in ER $[Ca^{2+}]$ but faster increase in $[Ca^{2+}]_i$ have been reported previously in cells treated with Tg or other SERCA inhibitors (30–32). In aggregate, SOCE appears to be fully activated at <50% depletion of the ER_{sub} (at this time point, there is a <15% decrease in $[Ca^{2+}]$ of the internal ER). These data agree well with the predictions made by the model.

ER stress response is a hallmark of global depletion of ER Ca^{2+} and has been reported to occur in cells treated with relatively high concentrations of Tg and agonists, within the range used to activate SOCE (33, 34). One of the earliest events in the unfolded protein response to ER stress is activation of the kinase PERK, which leads to inhibition of protein synthesis. Fig. 6*D* shows that PERK is activated within 3 min after stimulation with either 100 μM CCh or 1 μM Tg, detected as phosphorylated PERK. More significantly, treatment of cells with 1 μM Tg significantly increased cell death within 5 min (Fig. 6*E*; the effect of CCh on cell viability was not examined). However, low concentrations of Tg (1 and 10 nM) did not induce activation of PERK (Fig. 6*D*) or cell death for up to 15 min (Fig. 6*E*). Consistent with these findings, 1 μM Tg induced global redistribution of STIM1 into punctae following stimulation when compared with con-

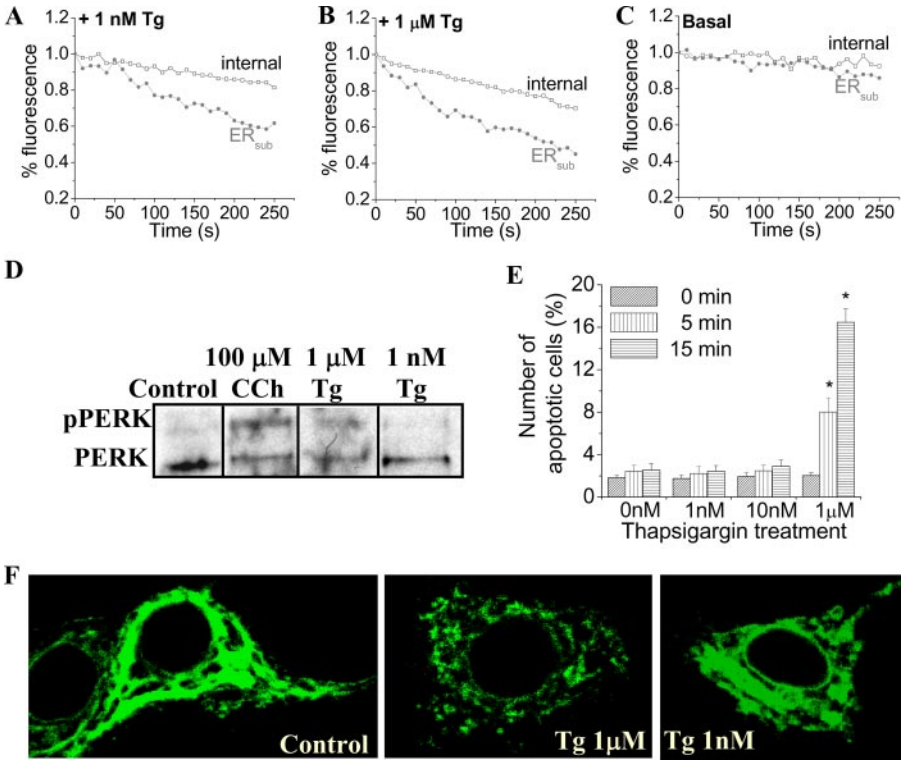

FIGURE 6. **Tg-stimulated depletion of ER Ca^{2+}.** [Ca^{2+}] in internal (*squares*) and subplasma membrane ER (ER_{sub}; *circles*) calcium stores in cells treated with 1 nM (*A*) or 1 μM Tg (*B*) and control cells (*C*) was measured using imaging of Mag-Fluo4 fluorescence. Confocal microscopy (details are given under "Experimental Procedures") was used to determine fluorescence changes. Fluorescence was determined in demarcated areas in the plasma membrane and internal regions (areas not shown). Traces shown are averages from at least 6–8 cells and represent similar data obtained from three separate experiments. *D*, detection of phosphorylated PERK (*pPERK*) in lysates of HSG cells treated with 100 μM CCh, 1 μM Tg, and 1 nM Tg by Western blotting using phospho-PERK antibody (1:1000 dilution). *E*, the percentage of apoptotic cells detected using the Vybrant staining assay in control HSG cells and cells treated with 1 nM, 10 nM, and 1 μM thapsigargin for 0, 5, and 15 min. Data are plotted as mean ± S.E., where an *asterisk* indicates $p < 0.05$. *F*, distribution of STIM1 in control HSG cells and following stimulation with 1 μM and 1 nM Tg. STIM1 was detected using the mouse anti-STIM1 antibody (1:100 dilution) and the fluorescein isothiocyanate-conjugated anti-mouse secondary antibody (1:100 dilution).

trol cells (Fig. 6*F*), whereas 1 nM induced minimal global redistribution of STIM1. It should be noted that 1 nM Tg does induce relocalization of STIM1 in the periphery of the cells (see Fig. 4). Similar results were also obtained using the muscarinic agonist CCh, which induces SOCE in HSG cells (1, 2, 16). Although global redistribution of STIM1 was observed following stimulation with 100 μM CCh, minimal redistribution was observed with 1 μM CCh (supplemental Fig. 2*A*). However, both high and low [CCh] induced peripheral STIM1 relocalization as detected by TIRFM (supplemental Fig. 2*B*). Previous reports show that low [agonist] and [IP_3] induce incomplete depletion of internal Ca^{2+} stores (14). However, TIRFM demonstrated that similar Ca^{2+} entry was induced by 300 nM and 10 μM CCh in exocrine gland acinar cells (35). Together, these data suggest that subplasma membrane ER depletion is involved in SOCE activation by CCh as well as Tg.

Localization of ER and Tg Stimulation of $[Ca^{2+}]_i$ Changes in the Subplasma Membrane Region—The data presented above strongly suggest that depletion of subplasma membrane ER is involved in relocalization of STIM1 and activation of SOCE. We measured this more directly using TIRFM. ER-Tracker Red dye labeling in this region as well as of the entire cytosol by epifluorescence (shown in Fig. 7*A*) conclusively demonstrated that ER is present in close proximity to the plasma membrane. These data agree well with recent studies reported by Lewis and co-workers (7, 8). Importantly, both 1 nM and 1 μM Tg induced sustained $[Ca^{2+}]_i$ increases in this region (Figs. 7, *B* and *C*; relative changes in Fluo-4 fluorescence measured using TIRFM are shown) in cells maintained in a normal Ca^{2+}-containing external medium. Fluorescence increase was greater and faster with the higher [Tg]. When 1 μM Gd^{3+} was included in the external solution to block SOCE, the increase was smaller and more transient in both cases (Fig. 7, *D* and *E*), suggesting that both Ca^{2+} release and Ca^{2+} entry contributed to the $[Ca^{2+}]_i$ increases seen in Fig. 7, *B* and *C*. However, internal Ca^{2+} release in the subplasma membrane region appears to be less when cells are treated with low Tg, since the change in Fluo-4 fluorescence induced by 1 μM Tg was faster and larger (Fig. 7*D*) that that seen with 1 nM Tg (Fig. 7*E*). A Ca^{2+} add-back protocol was used to measure SOCE (Fig. 7, *F* and *G*). The relative fluorescence changes induced by 1 nM and 1 μM Tg induced in a Ca^{2+}-free medium were similar to those seen in cells stimulated in the presence of 1 μM Gd^{3+} (note the difference in scale for traces compared with those used for Fig. 7, *B–E*). Importantly, the readdition of Ca^{2+} induced comparable increases in Fluo-4 fluorescence in cells treated with 1 μM and 1 nM Tg (Fig. 7, *F* and *G*), suggesting that similar SOCE was induced under these two conditions.

Mag-Fluo4 and TIRFM were used to confirm the depletion of peripheral Ca^{2+} stores by low and high [Tg]. As shown in Fig. 7*H*, both 1 nM and 1 μM Tg induced a similar decrease (about 50–60%) in Mag-Fluo4 fluorescence in the subplasma membrane regions in cells. Thus, peripheral ER depletion under these two conditions is similar. The apparently higher $[Ca^{2+}]_i$ increase in this region in 1 μM Tg-treated cells (Fig. 7, *B–E*) can be attributed to rapid diffusion of Ca^{2+} released more internally in the cells to the periphery (35).

DISCUSSION

The data presented above demonstrate that the peripheral relocalization of STIM1 and activation of SOCE are determined by the status of Ca^{2+} in ER localized in the subplasma membrane rather than in more internal regions of the cell. A key finding of this study is that low [Tg] (1 nM) activates SOCE to the same extent as high [Tg] (1 μM) but with much less internal Ca^{2+} store depletion. Importantly, the SOCE regulatory pro-

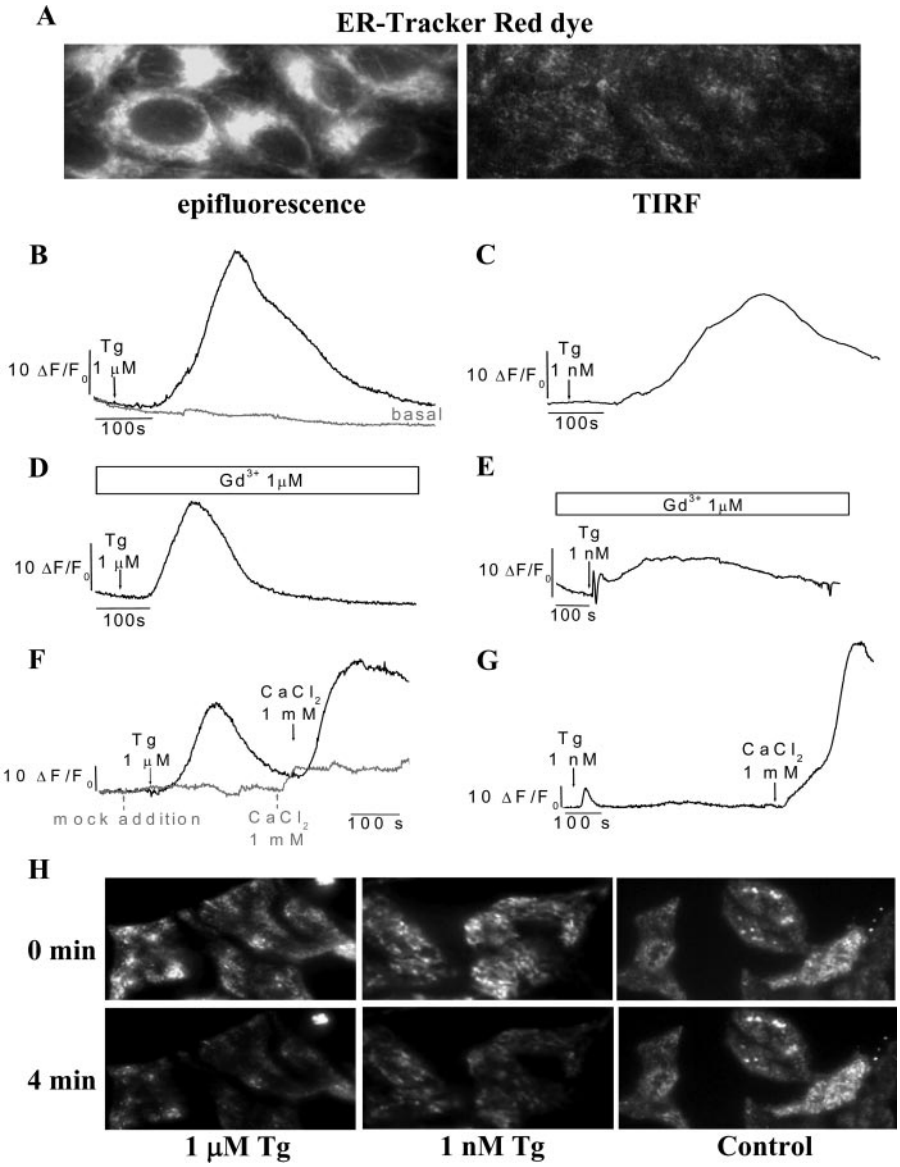

FIGURE 7. **Tg-stimulated [Ca^{2+}] changes in the subplasma membrane region.** *A*, localization of the ER network within the subplasma membrane region using the ER-Tracker Red dye; the *left* shows an epifluorescence image, and the *right* shows a TIRF image. TIRFM was used to monitor $[Ca^{2+}]_i$ with Fluo-4 (*B–G*) and [Ca^{2+}] in the ER with Mag-Fluo4 (*H*) fluorescence in the subplasma membrane region of HSG cells (details under "Experimental Procedures"). Each analog plot showing Ca^{2+} release and Ca^{2+} entry is representative of at least two experiments, with each trace showing the average for at least 20 cells. *B–E*, cells were stimulated with Tg in Ca^{2+}-containing medium, with or without 1 μM $GdCl_3$ (Gd^{3+}). Basal Ca^{2+} influx is as shown in *B*. *F* and *G*, cells were initially stimulated with thapsigargin (Tg) in Ca^{2+}-free medium, followed by the readdition of 1 mM $CaCl_2$ (fluorescence increase in each case was similar in the presence of Gd^{3+} or in Ca^{2+}-free medium; note that the scales in *F* and *G* are different from those in *B–E*). Basal Ca^{2+} influx is shown in *F*. *H*, cells were stimulated with Tg in Ca^{2+}-free medium. Images at 0 and 4 min after the Tg addition are as shown. For control cells, buffer was added instead of Tg.

tein STIM1 is relocalized primarily in the peripheral region of cells stimulated with 1 nM Tg in contrast to the more global relocation seen at the higher [Tg]. By using 1 nM BD-Tg to examine the extent of diffusion of Tg during activation of SOCE, we show that 1 nM Tg diffuses into the subplasma membrane region of the cells during the time required to maximally activate SOCE and relocalize STIM1 in this region. The presence of Tg in this region was temporally correlated with greater depletion of Ca^{2+} in ER localized in the periphery of the cells rather than in more internal regions. Finally, we show that under conditions where there is recycling of Ca^{2+} and incomplete depletion of peripheral ER, there is less mobilization of STIM1 in the subplasma membrane region. Ca^{2+}-induced Ca^{2+} release has been suggested to contribute to $[Ca^{2+}]_i$ increases, and specifically Ca^{2+} entry has been proposed to initiate Ca^{2+}-induced Ca^{2+} release in some cell types (28). However, we can rule out the involvement of Ca^{2+}-induced Ca^{2+} release in our findings based on the following: (i) Ba^{2+} entry was similar with 1 nM and 1 μM Tg; (ii) Mn^{2+} entry was also similar in both cases, although the onset of SOCE was slower at the lower [Tg]; (iii) blockers (ryanodine and caffeine; data not shown) of Ca^{2+}-induced Ca^{2+} release had no effect of 1 nM or 1 μM Tg-stimulated internal Ca^{2+} release or Ca^{2+} entry components; and (iv) Ca^{2+} entry measured by TIRF, which would exclude contributions of internal ER, was similar with 1 nM and 1 μM Tg. In aggregate, our data suggest that the formation of peripheral STIM1 punctae and SOCE activation is determined by the status of the local, subplasma membrane Ca^{2+} store and does not require depletion of more internal ER Ca^{2+} store. A decrease in the [Ca^{2+}] in the subplasma membrane ER is sensed by STIM1 localized within the same domain, which responds by redistributing into punctae. These STIM1 punctae have been suggested as the elemental functional unit of SOCE (7, 8) and probably represent homomeric complexes between STIM1 monomers as well as heteromeric interaction of STIM1 with proposed SOCE channels, TRPC1 and Orai1 (7, 9, 36–40). How exactly gating of the plasma membrane channel occurs is not yet clear, although STIM1 C terminus has been suggested to be sufficient for SOCE activation (9).

The juxtaposition of ER with the plasma membrane Ca^{2+} entry channel facilitates Ca^{2+} entering the cell to be rapidly taken up into these peripheral stores without a substantial change in the global $[Ca^{2+}]_i$. This allows the cell to control the $[Ca^{2+}]_i$ at the site of Ca^{2+} entry and thus minimize feedback inhibition of the channel by local increases in $[Ca^{2+}]_i$ (3–5). Thus, whereas uptake into the ER is dependent on the activity of SERCA pumps, retention of the Ca^{2+} within the ER is determined by its "leakiness." Our data demonstrate that the extent

of store depletion and therefore the time required for activation of SOCE as well as its magnitude is determined by recycling of Ca^{2+} into the ER, either from the cytosol or from the external medium via Ca^{2+} entry. When Ca^{2+} was used as the charge carrier, the lag for onset of the current was relatively longer with 1 nM Tg than with 1 μM Tg, and the magnitude of the current was also lower. However, when Na^+ was used as the charge carrier, (i) the magnitude of the current was similar in the two conditions, and (ii) although the lag with the lower [Tg] was reduced, it was still larger that that seen with 1 μM Tg. Similarly, Mn^{2+} entry was initially (<150 s) lower with 1 nM Tg. Further, we observed that I_{SOC} activated by low [Tg] was also relatively more stable than when stimulated by high [Tg]. These findings can be explained by the Ca^{2+} recycling that occurs at the lower [Tg] due to residual SERCA activity. Not only does this result in incomplete or delayed ER Ca^{2+} depletion, but it also lowers ambient $[Ca^{2+}]_i$ in the vicinity of the Ca^{2+} entry channel, thus attenuating Ca^{2+}-dependent feedback inhibition of the channel (1, 3, 19). An important finding that demonstrates the relevance of the peripheral ER store status is that at the lower [Tg], STIM1 relocation is more prominent in cells stimulated in medium without external Ca^{2+}. We suggest that under these conditions, Ca^{2+} in the peripheral stores is sufficiently depleted (*i.e.* concentration is below that required for optimal binding to STIM1) to cause STIM1 relocalization and SOCE activation.

Based on our findings, we propose that activation of SOCE is determined by the $[Ca^{2+}]$ in subplasma membrane ER. SOCE is activated by depletion of ER in this region and is not further increased by additional depletion of more internal ER. Our data also provide a possible explanation for activation of SOCE by agonist-dependent store depletion. Typically, low [agonist] induces $[Ca^{2+}]_i$ oscillations, which in some cases do not appear to be associated with SOCE (41), whereas higher [agonist] or $[IP_3]$ induces substantial ER depletion and maximally activates SOCE. We have shown here that low and high [CCh] induce similar relocation of STIM1 in the periphery of the cells, but only high [CCh] induces global relocation of STIM1. This indicates that low [CCh] probably induces depletion of peripheral but not internal ER. As suggested by our observations with Tg, small depletions of Ca^{2+} in the peripheral or internal ER might not lead to detectable SOCE due to rapid recycling of Ca^{2+}. However, higher $[IP_3]$ can induce substantial global Ca^{2+} depletion, resulting in SOCE that is easily detected. Consistent with this suggestion, Won and Yule (35) have demonstrated that Ca^{2+} entry induced by low concentrations of carbachol is not detectable using wide field microscopy but can be readily detected using TIRFM. In aggregate, our findings agree well with the mechanism proposed by Berridge (5) to describe how the Ca^{2+} status of peripheral and internal ER regulates SOCE, according to which depletion of peripheral ER or sufficient release of Ca^{2+} in the internal ER (enough to drain Ca^{2+} from the peripheral ER) can result in activation of SOCE. Further, the characteristic slow inactivation of SOCE that occurs as internal stores are refilled (6, 29, 42) can also be explained. Ca^{2+} entering the cell via SOCE is taken up into subplasma membrane ER, from where it diffuses into the internal ER if the latter is depleted. As the internal ER is refilled, $[Ca^{2+}]$ in the subplasma membrane ER will increase, resulting in inactivation of SOCE by an as yet unidentified mechanism. Whether this is correlated with STIM1 disaggregation is not yet known. As long as the internal ER stores are depleted, SOCE will remain activated. Thus, SOCE ensures refilling of internal Ca^{2+} stores, irrespective of the route of depletion, and protects against generation of ER stress and cell death.

In conclusion, STIM1, has been suggested to be an essential regulatory component of SOCE (7, 10–13). Studies reported recently have shown that stimulation of cells induces STIM1 to aggregate into punctae in the subplasma membrane region of the cells (7, 8, 10, 13), which appear to be causal in activation of SOCE. It is further suggested that these punctae indicate the localization of the functional unit of SOCE. The present data demonstrate that mobilization of STIM1 and activation of SOCE are associated with the decrease of Ca^{2+} in ER, which is localized within the subplasma region of the cell. Thus activation of SOCE by STIM1 is determined by the $[Ca^{2+}]$ in the peripheral Ca^{2+} store where STIM1 is also localized. As long as $[Ca^{2+}]$ in this store is below the threshold for binding to the STIM1 EF-hand domain, STIM1 will be localized in punctae, and SOCE will remain activated. Further studies are required to determine the exact molecular interactions involved in the generation of STIM1-containing punctae and how exactly these punctae regulate gating of the SOCE channel.

Acknowledgments—We are grateful to Dr. Tobias Meyer (Department of Molecular Pharmacology, Stanford University) for kindly providing the YFP-STIM1 DNA. We are also grateful to Dr. Vincent Schram (NICHD, National Institutes of Health) for assistance in TIRF, which was performed at the Microscopy and Imaging Core (NICHD, National Institutes of Health).

REFERENCES

1. Liu, X., and Ambudkar, I. S. (2001) *J. Biol. Chem.* **276,** 29891–29898
2. Liu, X., O'Connell, A., and Ambudkar, I. S. (1998) *J. Biol. Chem.* **273,** 33295–33304
3. Parekh, A. B. (2003) *J. Physiol.* (*Lond.*) **547,** 333–348
4. Ambudkar, I. S. (2004) *Sci. STKE 2004*, pe32
5. Berridge, M. (2004) *Sci. STKE 2004*, pe33
6. Putney, J. W., Jr. (1990) *Cell Calcium* **11,** 611–624
7. Luik, R. M., Wu, M. M., Buchanan, J., and Lewis, R. S. (2006) *J. Cell Biol.* **174,** 815–825
8. Wu, M. M., Buchanan, J., Luik, R. M., and Lewis, R. S. (2006) *J. Cell Biol.* **174,** 803–813
9. Huang, G. N., Zeng, W., Kim, J. Y., Yuan, J. P., Han, L., Muallem, S., and Worley, P. F. (2006) *Nat. Cell Biol.* **8,** 1003–1010
10. Liou, J., Kim, M. L., Heo, W. D., Jones, J. T., Myers, J. W., Ferrell, J. E., Jr., and Meyer, T. (2005) *Curr. Biol.* **15,** 1235–1241
11. Roos, J., DiGregorio, P. J., Yeromin, A. V., Ohlsen, K., Lioudyno, M., Zhang, S., Safrina, O., Kozak, J. A., Wagner, S. L., Cahalan, M. D., Velicelebi, G., and Stauderman, K. A. (2005) *J. Cell Biol.* **169,** 435–445
12. Spassova, M. A., Soboloff, J., He, L. P., Xu, W., Dziadek, M. A., and Gill, D. L. (2006) *Proc. Natl. Acad. Sci. U. S. A.* **103,** 4040–4045
13. Zhang, S. L., Yu, Y., Roos, J., Kozak, J. A., Deerinck, T. J., Ellisman, M. H., Stauderman, K. A., and Cahalan, M. D. (2005) *Nature* **437,** 902–905
14. Glitsch, M. D., and Parekh, A. B. (2000) *J. Physiol.* (*Lond.*) **523,** 283–290
15. Huang, Y., and Putney, J. W., Jr. (1998) *J. Biol. Chem.* **273,** 19554–19559
16. Liu, X., Singh, B. B., and Ambudkar, I. S. (2003) *J. Biol. Chem.* **278,** 11337–11343
17. Liu, X., Bandyopadhyay, B. C., Singh, B. B., Groschner, K., and Ambudkar, I. S. (2005) *J. Biol. Chem.* **280,** 21600–21606
18. Liu, X., Groschner, K., and Ambudkar, I. S. (2004) *J. Membr. Biol.* **200,**

93–104
19. Singh, B. B., Liu, X., Tang, J., Zhu, M. X., and Ambudkar, I. S. (2002) *Mol. Cell* **9,** 739–750
20. Harding, H. P., Zhang, Y., and Ron, D. (1999) *Nature* **397,** 271–274
21. Lockwich, T. P., Liu, X., Singh, B. B., Jadlowiec, J., Weiland, S., and Ambudkar, I. S. (2000) *J. Biol. Chem.* **275,** 11934–11942
22. Bandyopadhyay, B. C., Swaim, W. D., Liu, X., Redman, R. S., Patterson, R. L., and Ambudkar, I. S. (2005) *J. Biol. Chem.* **280,** 12908–12916
23. Liu, X., Singh, B. B., and Ambudkar, I. S. (1999) *J. Biol. Chem.* **274,** 25121–25129
24. Bollimuntha, S., Singh, B. B., Shavali, S., Sharma, S. K., and Ebadi, M. (2005) *J. Biol. Chem.* **280,** 2132–2140
25. Ong, H. L., Liu, X., Sharma, A., Hegde, R. S., and Ambudkar, I. S. (2007) *Pfluegers Arch. Eur. J. Physiol.* **453,** 797–808
26. Parekh, A. B., and Putney, J. W., Jr. (2005) *Physiol. Rev.* **85,** 757–810
27. Putney, J. W., Jr. (2001) *Mol. Intervent.* **1,** 84–94
28. Yao, J., Li, Q., Chen, J., and Muallem, S. (2004) *J. Biol. Chem.* **279,** 21511–21519
29. Mertz, L. M., Baum, B. J., and Ambudkar, I. S. (1990) *J. Biol. Chem.* **265,** 15010–15014
30. Burdakov, D., Petersen, O. H., and Verkhratsky, A. (2005) *Cell Calcium* **38,** 303–310
31. Landolfi, B., Curci, S., Debellis, L., Pozzan, T., and Hofer, A. M. (1998) *J. Cell Biol.* **142,** 1235–1243
32. Lee, M. Y., Song, H., Nakai, J., Ohkura, M., Kotlikoff, M. I., Kinsey, S. P., Golovina, V. A., and Blaustein, M. P. (2006) *Proc. Natl. Acad. Sci. U. S. A.* **103,** 13232–13237
33. Brostrom, M. A., and Brostrom, C. O. (2003) *Cell Calcium* **34,** 345–363
34. Paschen, W. (2001) *Cell Calcium* **29,** 1–11
35. Won, J. H., and Yule, D. I. (2006) *Am. J. Physiol.* **291,** G146–G155
36. Mercer, J. C., Dehaven, W. I., Smyth, J. T., Wedel, B., Boyles, R. R., Bird, G. S., and Putney, J. W., Jr. (2006) *J. Biol. Chem.* **281,** 24979–24990
37. Peinelt, C., Vig, M., Koomoa, D. L., Beck, A., Nadler, M. J., Koblan-Huberson, M., Lis, A., Fleig, A., Penner, R., and Kinet, J. P. (2006) *Nat. Cell Biol.* **8,** 771–773
38. Soboloff, J., Spassova, M. A., Tang, X. D., Hewavitharana, T., Xu, W., and Gill, D. L. (2006) *J. Biol. Chem.* **281,** 20661–20665
39. Vig, M., Peinelt, C., Beck, A., Koomoa, D. L., Rabah, D., Koblan-Huberson, M., Kraft, S., Turner, H., Fleig, A., Penner, R., and Kinet, J. P. (2006) *Science* **312,** 1220–1223
40. Smyth, J. T., Dehaven, W. I., Jones, B. F., Mercer, J. C., Trebak, M., Vazquez, G., and Putney, J. W., Jr. (2006) *Biochim. Biophys. Acta* **1763,** 1147–1160
41. Petersen, O. H. (2002) *Biol. Res.* **35,** 177–182
42. Parekh, A. B., and Penner, R. (1997) *Physiol. Rev.* **77,** 901–930

Mechanisms of Signal Transduction:

Relocalization of STIM1 for Activation of Store-operated Ca^{2+} Entry Is Determined by the Depletion of Subplasma Membrane Endoplasmic Reticulum Ca^{2+} Store

Hwei Ling Ong, Xibao Liu, Krasimira Tsaneva-Atanasova, Brij B. Singh, Bidhan C. Bandyopadhyay, William D. Swaim, James T. Russell, Ramanujan S. Hegde, Arthur Sherman and Indu S. Ambudkar

J. Biol. Chem. 2007, 282:12176-12185.
doi: 10.1074/jbc.M609435200 originally published online February 12, 2007
